

Mononuclear Thiomolybdenyl Complexes – Synthesis and Structural and Spectroscopic Characterization

Charles G. Young,^{*,[a]} Robert W. Gable,^[a] Jason P. Hill,^[a] and Graham N. George^[b]

Keywords: Molybdenum / Sulfur / Thiomolybdenyl complexes / EPR spectroscopy / X-ray absorption spectroscopy

The first series of mononuclear thiomolybdenyl complexes, $\text{Tp}^*\text{Mo}^{\text{V}}\text{SX}_2$ [Tp^* = hydrotris(3,5-dimethylpyrazol-1-yl)borate, X/X_2 = anion/dianion], has been prepared. The complexes, which have been characterized by analytical, mass

spectrometric, spectroscopic and X-ray crystallographic studies, provide insights into the electronic nature and chemistry of the catalytically and biologically important thiomolybdenyl unit.

Introduction

The thiomolybdenyl unit, $\{\text{Mo}^{\text{V}}=\text{S}\}^{3+}$, has been implicated in the turnover of industrial catalysts^[1,2] and mononuclear, pterin-containing molybdenum enzymes such as xanthine oxidase and aldehyde oxidase.^[3–6] However, mononuclear thiomolybdenyl complexes are extremely rare due to their susceptibility to redox, polynucleation, and hydrolysis reactions.^[3–6] Consequently, our understanding of their chemical, structural, and spectroscopic characteristics is very limited. This stands in stark contrast to well advanced studies of molybdenyl, $\{\text{Mo}^{\text{V}}=\text{O}\}^{3+}$, complexes.^[7–17] Indeed, only two mononuclear thiomolybdenyl complexes have ever been isolated and completely characterized. The first of these, $\text{Tp}^*\text{Mo}^{\text{V}}\text{SCl}_2$ [Tp^* = hydrotris(3,5-dimethylpyrazol-1-yl)borate], was reported by Young et al. in 1987.^[18] This complex was prepared by treating $\text{Tp}^*\text{MoOCl}_2$ with boron sulfide and has been characterized by infrared, UV-visible, electron paramagnetic resonance (EPR), Raman, and X-ray absorption (XAS) and extended X-ray absorption fine structure (EXAFS) spectroscopy.^[18–21] Crystallographic characterization of the compound has not been attempted due to the high probability of disorder of the thio and chloro ligands.^[22] A number of related complexes, viz., $[\text{Tp}^*\text{MoS}(\text{S}_2\text{PR}_2)]^+$ and $[\text{Tp}'\text{MoS}(\text{S}_2\text{PR}_2)]^+$ [Tp' = hydrobis(3-isopropylpyrazol-1-yl)(5-isopropylpyrazol-1-yl)borate] have been generated in solution.^[23,24] Recently, a second mononuclear thiomolybdenyl complex, $\text{Mo}^{\text{V}}\text{S}(\text{N}[\text{R}]\text{Ar})_3$ $\{\text{N}[\text{R}]\text{Ar} = \text{N}[\text{C}(\text{CD}_3)_2\text{CH}_3](3,5\text{-Me}_2\text{C}_6\text{H}_3)\}$, was reported by Johnson et al.^[25] This complex, a member of the series $\text{MoE}(\text{N}[\text{R}]\text{Ar})_3$ ($\text{E} = \text{O}, \text{S}, \text{Se}, \text{Te}$), was prepared by oxidizing $\text{Mo}(\text{N}[\text{R}]\text{Ar})_3$ with S_8 or ethylene sulfide. The $\text{MoE}(\text{N}[\text{R}]\text{Ar})_3$ complexes exhibit rhombic EPR spectra with A_{Mo} values decreasing in the order $\text{Mo}=\text{O} > \text{Mo}=\text{S} > \text{Mo}=\text{Se}$

$> \text{Mo}=\text{Te}$, consistent with increasing covalency in complexes of the heavier chalcogenides. The crystal structure of $\text{MoS}(\text{N}[\text{R}]\text{Ar})_3$ revealed a distorted tetrahedral complex possessing a terminal thio ligand with an $\text{Mo}=\text{S}$ distance of 2.1677(12) Å.

Synthetic access to a series of related thiomolybdenyl complexes would permit systematic spectroscopic and structural studies leading to a detailed electronic description of the $\{\text{Mo}^{\text{V}}=\text{S}\}^{3+}$ unit and insights into its vital roles in industrial and biological catalysis. We report here the synthesis and characterization of the complexes $\text{Tp}^*\text{Mo}^{\text{V}}\text{SX}_2$ [$\text{X} = \text{OPh}$, 2-(ethylthio)phenolate (etp), 2-(*n*-propyl)phenolate (pp); $\text{X}_2 = \text{benzene-1,2-diolate (cat)}$, 4-methylbenzene-1,2-dithiolate (tdt), benzene-1,2-dithiolate (bdt)] and the crystal structures of $\text{Tp}^*\text{MoS}(\text{etp})_2$ and $\text{Tp}^*\text{MoS}(\text{bdt})$; the latter, features a pseudo-dithiolene co-ligand and is of direct relevance to molybdoenzyme intermediates such as the Very Rapid centre of xanthine oxidase, proposed to contain an $[\text{Mo}^{\text{V}}\text{OS}(\text{dithiolene})]^-$ moiety.^[3–6]

Results and Discussion

We have employed two general methods in the generation of Tp^*MoSX_2 complexes. The first, the reaction of Tp^*MoOX_2 ^[9] with boron sulfide, is useful for the generation of species in situ (as demonstrated by EPR spectroscopy) but does not lend itself to isolation of the compounds. The second method, metathesis of $\text{Tp}^*\text{MoSCl}_2$ ^[18] with salts of X^- or X_2^{2-} , permits the isolation of pure Tp^*MoSX_2 (e.g., $\text{X} = \text{OPh}$, etp, pp; $\text{X}_2 = \text{cat}$, bdt, tdt) following workup. The reactions are conveniently monitored by EPR spectroscopy, which reveals the clean replacement of $\text{Tp}^*\text{MoSCl}_2$ by product in reaction times of 2 to 16 h. Rapid anaerobic work-up, including volume reduction and passage through a short bed of silica, is essential to the isolation of pure products. As solids the compounds are moderately air-stable but recrystallizations and solution studies must be performed under strictly anaerobic conditions. The stability of the thiomolybdenyl complexes appears to be enhanced by the presence of very bulky *O*-donor co-ligands, such as

^[a] School of Chemistry, University of Melbourne, Victoria 3010, Australia
Fax: (internat.) +61 (0)3 9347 5180
E-mail: cgyoung@unimelb.edu.au

^[b] Stanford Synchrotron Radiation Laboratory, SLAC, P. O. Box 4349, MS 69, Stanford, CA 94309, U.S.A.

etp and pp, or chelate ligands. The complexes have been characterized by microanalytical, mass spectrometric and spectroscopic methods. Clean electron-impact mass spectra with strong parent ions are observed for the more stable (etp, pp, cat, tdt, bdt) derivatives. The IR spectra of the complexes exhibit a single, strong $\nu(\text{Mo}=\text{S})$ band in the range $505\text{--}490\text{ cm}^{-1}$, as well as bands characteristic of Tp^* and the *O*- or *S*-donor co-ligands.

The structures of $\text{Tp}^*\text{MoS}(\text{etp})_2$ and $\text{Tp}^*\text{MoS}(\text{bdt})$ have been determined by X-ray crystallography and ORTEP diagrams are given in Figure 1 and Figure 2, respectively. The distorted octahedral complexes contain a terminal thio ligand, two monodentate *O*-donor ligands (etp) or a bidentate, dithiolenic, *S*-donor ligand (bdt), and a facial, tridentate Tp^* ligand. The $\text{Mo}\text{--}\text{S}(1)$ distances of $2.1279(10)\text{ \AA}$ and $2.1231(11)\text{ \AA}$, respectively, are typical of $\text{Mo}=\text{S}$ units observed in $\text{MoS}(\text{N}[\text{R}]\text{Ar})_3$ ^[25] and polynuclear complexes.^[26] For $\text{Tp}^*\text{MoS}(\text{etp})_2$, the $\text{Mo}\text{--}\text{O}(4)$ and $\text{Mo}\text{--}\text{O}(5)$ distances are $1.953(2)\text{ \AA}$ and $1.951(2)\text{ \AA}$ and the associated $\text{Mo}\text{--}\text{O}\text{--}\text{C}$ angles are $140.9(2)^\circ$ and $134.4(2)^\circ$, respectively. The Mo atom lies $0.264(1)\text{ \AA}$ out of the plane of the $\text{O}(4)$, $\text{O}(5)$, $\text{N}(21)$ and $\text{N}(31)$ atoms toward the thio ligand and the $\text{S}(1)\text{--}\text{Mo}\text{--}\text{O}$ angles are consequently opened to ca. 103° . The $\text{Mo}\text{--}\text{N}(n1)$ distances are dictated by the relative *trans* influences of the co-ligands, the $\text{Mo}\text{--}\text{N}(11)$ distance being lengthened by $0.104(6)\text{ \AA}$ relative to the other $\text{Mo}\text{--}\text{N}$ bonds. A very similar *trans* influence of $0.105(5)\text{ \AA}$ is observed for $\text{Tp}^*\text{MoO}(\text{etp})_2$.^[27] For $\text{Tp}^*\text{MoS}(\text{bdt})$, the $\text{Mo}\text{--}\text{S}(4)$ and $\text{Mo}\text{--}\text{S}(5)$ distances are $2.3704(12)\text{ \AA}$ and $2.3668(12)\text{ \AA}$, respectively, and the associated $\text{Mo}\text{--}\text{S}\text{--}\text{C}$ angles are ca. 104.2° . The Mo atom lies $0.296(1)\text{ \AA}$ out of the plane of the $\text{S}(4)$, $\text{S}(5)$, $\text{N}(21)$, and $\text{N}(31)$ atoms and $0.592(7)\text{ \AA}$ out of the plane of the bdt ligand, toward the thio ligand. The $\text{Mo}\text{--}\text{N}(11)$ distance is lengthened by ca. 0.2 \AA relative to the other two $\text{Mo}\text{--}\text{N}$ bonds. A comparatively large *trans* influence has also been observed for $\text{Tp}^*\text{MoO}(\text{catCl}_4)$ ($\text{catCl}_4 = 1,2,3,4\text{-tetrachlorobenzene-5,6-diolate}$)^[12] and $\text{Tp}^*\text{MoO}(\text{bdt})$;^[13] steric interaction between bidentate ligands and the nearby 3-methyl group [C(11) in Figure 2] accounts for this lengthening as well as the discernable bend in the MoX_2 fragment about the $\text{E}\cdots\text{E}$ vector ($\text{E} = \text{O}, \text{S}$) (such that the benzene ring moves away from said methyl group). In the thiomolybdenyl complexes, there are no interactions between the terminal thio ligand and co-ligand sulfur atoms, the $\text{S}\cdots\text{S}$ distances ($> 4.5\text{ \AA}$) being considerably larger than the van der Waals contact distance.

Related structures for the other members of the series have been established by molybdenum and sulfur K-edge XAS and EXAFS studies. MoK -edge EXAFS spectra exhibit a strong backscattering component consistent with the presence of a thiomolybdenyl unit, with $\text{Mo}=\text{S}$ distances in the range $2.1\text{--}2.2\text{ \AA}$. Intense pre-edge features are seen in the S K-edge X-ray absorption spectra of the compounds (Figure 3). The most intense feature, at ca. 2466 eV , is characteristic of terminal thio ligation and is assigned to $\text{S}(1s)\rightarrow\text{Mo}=\text{S}\pi^*$ transitions.^[19] In each case, the pre-edge feature is broader than expected based on the experimental resolution and deconvolution of the band provides evidence

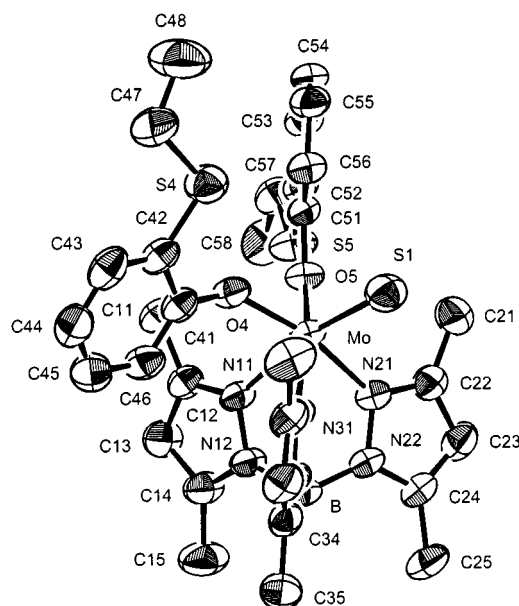


Figure 1. Molecular structure of $\text{Tp}^*\text{MoS}(\text{etp})_2$. Additional bond lengths [\AA] and angles [$^\circ$]: $\text{Mo}\text{--}\text{N}(11)$ $2.279(3)$, $\text{Mo}\text{--}\text{N}(21)$ $2.174(3)$, $\text{Mo}\text{--}\text{N}(31)$ $2.175(3)$; $\text{S}(1)\text{--}\text{Mo}\text{--}\text{O}(4)$ $104.20(8)$, $\text{S}(1)\text{--}\text{Mo}\text{--}\text{O}(5)$ $101.11(7)$, $\text{S}(1)\text{--}\text{Mo}\text{--}\text{N}(11)$ $168.28(7)$, $\text{S}(1)\text{--}\text{Mo}\text{--}\text{N}(21)$ $91.01(8)$, $\text{S}(1)\text{--}\text{Mo}\text{--}\text{N}(31)$ $92.81(8)$, $\text{O}(4)\text{--}\text{Mo}\text{--}\text{O}(5)$ $89.96(9)$

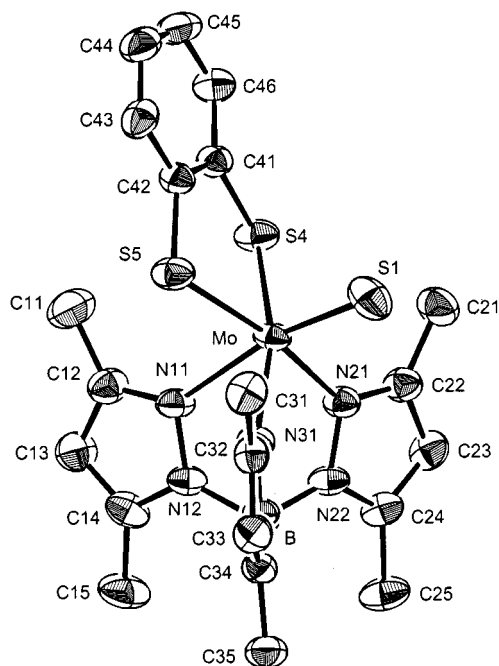


Figure 2. Molecular structure of $\text{Tp}^*\text{MoS}(\text{bdt})$. Additional bond lengths [\AA] and angles [$^\circ$]: $\text{Mo}\text{--}\text{N}(11)$ $2.393(3)$, $\text{Mo}\text{--}\text{N}(21)$ $2.201(3)$, $\text{Mo}\text{--}\text{N}(31)$ $2.189(3)$; $\text{S}(1)\text{--}\text{Mo}\text{--}\text{S}(4)$ $101.24(5)$, $\text{S}(1)\text{--}\text{Mo}\text{--}\text{S}(5)$ $100.99(5)$, $\text{S}(1)\text{--}\text{Mo}\text{--}\text{N}(11)$ $168.93(8)$, $\text{S}(1)\text{--}\text{Mo}\text{--}\text{N}(21)$ $92.88(9)$, $\text{S}(1)\text{--}\text{Mo}\text{--}\text{N}(31)$ $95.09(9)$, $\text{S}(4)\text{--}\text{Mo}\text{--}\text{S}(5)$ $83.84(8)$

for several transitions, probably to nearly degenerate $\text{Mo}=\text{S}\pi^*$ orbitals with S *p* and Mo d_{xz} and d_{yz} orbital character (*z* along $\text{Mo}=\text{S}$). For example, deconvolution of the spectrum of $\text{Tp}^*\text{MoS}(\text{pp})_2$ (Figure 3, a) reveals transitions at

2466.3 and 2467.0 eV. The precise origin of these and related transitions is currently under further experimental and theoretical interrogation. Similar pre-edge features are observed in the S K XAS spectra of $\text{Tp}^*\text{MoSCl}_2$ ^[28,29] and $\text{Tp}^*\text{MoOS(OPh)}$ [Tp^* = hydrotris(3-isopropylpyrazol-1-yl)borate].^[29] These complexes exhibit three distinct S K pre-edge features at energies different to those of the thiomolybdenyl complexes (around 2466.1, 2467.7 and 2469.6 eV compared to 2466 and 2469 eV for the thiomolybdenyl complexes). The feature at 2469 eV is tentatively assigned to a sulfur $1s \rightarrow \sigma^*$ transition associated with the Mo=S unit.

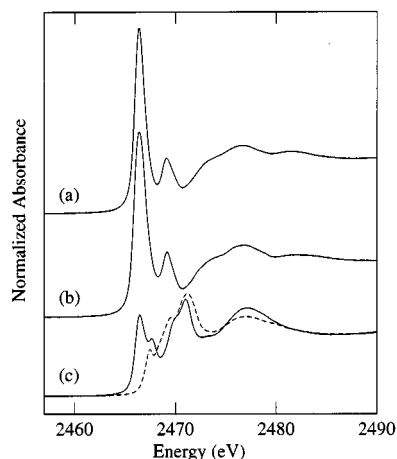


Figure 3. Selected sulfur K-edge X-ray absorption spectra of solids at 293 K. (a) $\text{Tp}^*\text{MoS(pp)}_2$, (b) $\text{Tp}^*\text{MoS(cat)}$, (c) $\text{Tp}^*\text{MoS(bdt)}$, overlaid with the (dashed) spectrum of $\text{Tp}^*\text{MoO(bdt)}$

The thiomolybdenyl complexes are EPR-active and generally exhibit highly anisotropic monoclinic frozen-glass EPR spectra (Table 1), with g_{iso} values substantially lower than their oxo analogues.^[9] This results from a lowering of all the g tensor components, particularly g_3 , rather than any change in the sense of the anisotropy. Very similar EPR parameters, with an unusually low g_3 and consequently high g anisotropy, characterize the three available $\text{Tp}^*\text{MoS(OR)}_2$ complexes. These complexes exhibit relatively large A_{iso} values around $46 \times 10^{-4} \text{ cm}^{-1}$. As a group, they also exhibit similar electronic spectra with intense LMCT absorptions in the regions 465–509 nm and 354–400 nm, and a d–d band at ca. 1300 nm (ϵ ca. $100 \text{ M}^{-1} \cdot \text{cm}^{-1}$, cf. d–d band at 800 nm in oxo analogues^[9,18]). Expressions for the principal g tensor components for compounds of this type have been presented;^[18] the decrease in the tensor components is ascribed to a decrease in the energies of the ground to excited-state d–d transitions, most importantly $(d_{x^2-y^2})^1 \rightarrow (d_{xz})^1$ and $(d_{x^2-y^2})^1 \rightarrow (d_{yz})^1$, as a consequence of the weaker ligand field of the thio ligand. The similar A_{Mo} values for the Tp^*MoSX_2 ($X = \text{Cl}, \text{OR}$) complexes implies an essentially similar ground state electronic configuration [viz., $(d_{x^2-y^2})^1$] with a similar degree of Mo–X covalency. The EPR spectrum of $\text{Tp}^*\text{MoS(cat)}$, which contains a pseudo ene-1,2-diolate moiety, differs dramatically from those of the $\text{Tp}^*\text{MoS(OR)}_2$ complexes; for $\text{Tp}^*\text{MoS-}$

(cat), g_1 and g_2 are very similar and g_{iso} is consequently increased compared to $\text{Tp}^*\text{MoS(OR)}_2$. Similar “chelate effects” have been observed for analogous oxo complexes and may be ascribed to an increase in the energy of ground to excited-state transitions as a consequence of $p\pi - d\pi$ interactions.^[10] Higher g_{iso} and lower A_{iso} parameters characterize the thiolate complexes $\text{Tp}^*\text{MoS(SPh)}_2$, $\text{Tp}^*\text{MoS(bdt)}$, and $\text{Tp}^*\text{MoS(tdt)}$, with the chelate complexes again exhibiting a higher g_{iso} than the non-chelated complex. The electronic spectra of $\text{Tp}^*\text{MoS(cat)}$, $\text{Tp}^*\text{MoS(SPh)}_2$, and $\text{Tp}^*\text{MoS(tdt)}$ exhibit intense charge transfer bands only in accessible spectral regions; a near-IR absorption around 1300 nm is not observed. A multi-frequency EPR study of the compounds is currently underway.

Table 1. Selected EPR parameters (A values $\times 10^{-4} \text{ cm}^{-1}$)

Compound	g_1	g_2	g_3	g_{iso}	Δg_i	A_{iso}
$\text{Tp}^*\text{MoSCl}_2$ ^[18]	1.941	1.921	1.919	1.928	0.022	46.8
$\text{Tp}^*\text{MoS(etp)}_2$	1.961	1.914	1.864	1.909	0.097	46.6
$\text{Tp}^*\text{MoS(pp)}_2$	1.956	1.909	1.858	1.902	0.098	46.6
$\text{Tp}^*\text{MoS(OPh)}_2$	1.955	1.913	1.860	1.900	0.095	46.8
$\text{Tp}^*\text{MoS(cat)}$	1.960	1.960	1.900	1.934	0.060	38.9
$\text{Tp}^*\text{MoS(SPh)}_2$ ^[a]	1.993	1.945	1.910	1.940	0.083	36.8
$\text{Tp}^*\text{MoS(tdt)}$	2.000	1.971	1.919	1.956	0.081	36.9
$\text{Tp}^*\text{MoS(bdt)}$	1.996	1.968	1.915	1.960	0.081	36.6

[a] Generated in situ, not isolated.

Success in derivatizing $\text{Tp}^*\text{MoSCl}_2$ has provided synthetic access to a variety of thiomolybdenyl complexes of the type Tp^*MoSX_2 . These are currently the focus of systematic structural and spectroscopic, especially EPR, MCD, XAS, and EXAFS, studies aimed at elucidating the electronic structure of thiomolybdenyl and related units and understanding their roles in industrial and biological catalysis.

Experimental Section

General: All syntheses and solution studies were carried out under an atmosphere of dinitrogen using dried, deoxygenated, and distilled solvents. The method of Young et al.^[18] was employed in the synthesis of $\text{Tp}^*\text{MoSCl}_2$. The course of metathesis reactions were monitored using EPR spectroscopy and work-up was initiated upon complete conversion of $\text{Tp}^*\text{MoSCl}_2$ to product. – Chromatographic separations and purifications were performed under dinitrogen using dried, deoxygenated solvents and Merck Art 7734 Kieselgel 60. Spectroscopic studies were carried out under strictly anaerobic conditions. – Mass spectra were obtained on a JOEL JMS-AX505H mass spectrometer. – Infrared spectra were recorded on a BIO-RAD FTS-165 FTIR spectrophotometer as pressed KBr discs. – EPR spectra were run on a Bruker ECS 106 ESR spectrometer, equipped with a flow through low temperature device, allowing frozen spectra to be recorded at approximately 120 K. The spectral parameters in Table 1 were obtained by inspection. – Electronic spectra were obtained on a Hitachi 150-20 spectrophotometer. – Microanalyses were performed by Atlantic Microlabs, Norcross, GA, USA.

$\text{Tp}^*\text{MoS(etp)}_2$: 2-Ethylthiophenol (0.18 cm³, 1.01 mmol) and triethylamine (0.15 cm³, 1.01 mmol) were added to a stirred solution

of $\text{Tp}^*\text{MoSCl}_2$ (250 mg, 0.5 mmol) in dichloromethane (30 cm^3). The solution rapidly turned a purple color, then became brown. After 4 h the volume of the solution was reduced by half and it was filtered through a bed (4–5 cm) of silica gel. The bed of silica was washed with dichloromethane (30 cm^3), then the combined filtrate and washings were reduced to a minimum volume and treated (dropwise) with methanol to precipitate the red crystalline product. Yield 150 mg (41%).

$\text{C}_{31}\text{H}_{40}\text{BMoN}_6\text{O}_2\text{S}_3$ (731.6): calcd. C 50.89, H 5.51, N 11.49, S 13.15; found C 51.06, H 5.27, N 11.69, S 13.30. – IR (KBr): $\tilde{\nu}$ = 2525, m, $\nu(\text{BH})$; 1570, m; 1541, s, $\nu(\text{CN})$; 1459, s; 1364, s; 1261, s; 1201, s; 1068, s; 857, s; 748, s; 693, s; 615, s; 500, s, $\nu(\text{Mo}=\text{S})$. – Mass Spec: m/z $[\text{M} - \text{H}]^+$ 732.

$\text{Tp}^*\text{MoS}(\text{bdt})$: 1,2-Benzenedithiol (0.1 cm^3 , 0.90 mmol) and triethylamine (0.29 cm^3 , 1.90 mmol) were added to a stirred solution of $\text{Tp}^*\text{MoSCl}_2$ (450 mg, 0.90 mmol) in dichloromethane (30 cm^3). The solution rapidly turned a red color and after 2 h the volume of the solution was reduced to a minimum, filtered through a short bed of silica and recrystallized as described above for $\text{Tp}^*\text{MoS}(\text{etp})_2$. The yield of red crystals was 220 mg (43%). The analytical sample was purified by anaerobic column chromatography on silica gel using 3:2 dichloromethane/hexane as eluent, then recrystallized from dichloromethane/methanol.

$\text{C}_{21}\text{H}_{26}\text{BMoN}_6\text{S}_3 \cdot 0.5\text{CH}_3\text{OH}$ (581.4): calcd. C 44.41, H 4.85, N 14.45, S 16.54; found: C 44.02, H 4.77, N 14.40, S 16.49. – IR (KBr): $\tilde{\nu}$ = 2557, m, $\nu(\text{BH})$; 1540, s, $\nu(\text{CN})$; 1447, s; 1435, s; 1412, s; 1357, s; 1262, m; 1202, s; 1093, m; 1074, s; 1036, s; 854, m; 814, m; 790, s; 745, s; 692, m; 666, w; 647, w; 499, s, $\nu(\text{Mo}=\text{S})$ cm^{-1} . – Mass Spec: m/z $[\text{M} + \text{H}]^+$ 568.

The other members of the series were prepared by essentially similar methods.

Crystal Structure Determination for $\text{Tp}^*\text{MoS}(\text{etp})_2$: Crystallographic data: $\text{C}_{31}\text{H}_{40}\text{BMoN}_6\text{O}_2\text{S}_3$, $M = 731.65$, triclinic, $P\bar{1}$, $a = 10.825(2)$, $b = 11.584(2)$, $c = 14.428(2)$ Å, $\alpha = 86.735(11)$, $\beta = 88.669(12)$, $\gamma = 71.998(13)^\circ$, $V = 1717.8(5)$ Å³, $d_c = 1.414$ g·cm⁻³, $Z = 2$. A total of 6039 unique data with 4871 reflections having $I > 2\sigma(I)$ were collected. The structure was solved by Patterson and direct methods (SHELXS-86)^[30] and was refined on F^2 by a full-matrix least-squares procedure (SHELXL-97)^[31] using all data. All hydrogens were included at geometrical estimates. R_1 [$I > 2\sigma(I)$] = 0.0390 and wR_2 (all data) = 0.0998. Figure 1 and Figure 2 were prepared using the program ORTEP.^[32]

Crystal Structure Determination for $\text{Tp}^*\text{MoS}(\text{bdt})$: Crystallographic data: $\text{C}_{21}\text{H}_{26}\text{BMoN}_6\text{S}_3$, $M = 565.43$, monoclinic, $P2_1/n$, $a = 10.0296(13)$, $b = 14.729(2)$, $c = 16.846(2)$ Å, $\beta = 95.456(10)^\circ$, $V = 2477.3(6)$ Å³, $d_c = 1.516$ g·cm⁻³, $Z = 4$. A total of 4346 unique data with 2922 reflections having $I > 2\sigma(I)$ were collected and the structure was solved as described above. R_1 [$I > 2\sigma(I)$] = 0.0346 and wR_2 (all data) = 0.0967.

Crystallographic data (excluding structure factors) for the structures reported in this paper have been deposited with the Cambridge Crystallographic Data Centre as supplementary publications nos. CCDC-157193 and CCDC-157194. Copies of the data can be obtained free of charge on application to CCDC, 12 Union Road, Cambridge CB2 1EZ, UK [Fax: (internat.) +44–1223/336-033; E-mail: deposit@ccdc.cam.ac.uk].

X-ray Absorption Spectroscopy: X-ray absorption spectroscopy was carried out at the Stanford Synchrotron Radiation Laboratory with the SPEAR storage ring containing 60–100 mA at 3.0 GeV. Mol-

ybdenum K-edge spectra were collected on beamline 7–3 using a Si(220) double crystal monochromator with an upstream vertical aperture of 1 mm and a wiggler field of 1.8 T. Harmonic rejection was accomplished by detuning one monochromator crystal to approximately 60% off-peak. X-ray absorption was measured in transmittance using nitrogen-filled ionization chambers. The spectrum of molybdenum foil was collected simultaneously with that of the sample and data were calibrated with reference to the lowest energy inflection point of the standard (assumed to be 20003.9 eV). Samples were prepared in a boron nitride matrix and during data collection were maintained at a temperature of approximately 10 K using an Oxford Instruments liquid helium flow cryostat.

Sulfur K edge experiments were performed on beamline 6–2 using an Si(111) double crystal monochromator and wiggler field of 1.0 T. Harmonic rejection was accomplished by using a flat nickel coated mirror downstream of the monochromator adjusted so as to have a cutoff energy of about 4500 eV. Incident intensity was monitored using an ion chamber contained in a (flowing) helium-filled flight path. X-ray absorption was monitored by recording total electron yield and the energy scale was calibrated with reference to the lowest energy peak of the sodium thiosulfate standard ($\text{Na}_2\text{S}_2\text{O}_3 \cdot 5\text{H}_2\text{O}$) which was assumed to be 2469.2 eV. Samples were examined at ambient temperature. Peak positions in near-edge spectra were estimated by curve-fitting to a sum of pseudo-Voigt peaks using the program EDG FIT (pseudo-Voigt deconvolution).^[33]

Acknowledgments

We gratefully acknowledge the financial support of the Australian Research Council and the Australian Department of Industry, Science and Technology. SSRL is funded by the Department of Energy (DOE) BES, with further support by DOE OBER and the NIH.

- [1] E. G. Derouane, E. Pedersen, B. S. Clausen, Z. Gabelica, H. Topsøe, *J. Catal.* **1987**, *107*, 587–588.
- [2] M. Rakowski DuBois, *Chem. Rev.* **1989**, *89*, 1–9.
- [3] R. Hille, *Chem. Rev.* **1996**, *96*, 2757–2816.
- [4] R. S. Pilato, E. I. Stiefel, in: *Bioinorganic Catalysis* (Ed.: J. Reedijk, E. Bouwman), Marcel Dekker, New York, **1999**, 2nd ed., p. 81–152.
- [5] J. H. Enemark, C. G. Young, *Adv. Inorg. Chem.* **1993**, *40*, 1–88.
- [6] C. G. Young, *J. Biol. Inorg. Chem.* **1997**, *2*, 810–816.
- [7] H. B. Gray, C. R. Hare, *Inorg. Chem.* **1962**, *1*, 363–368.
- [8] G. R. Hanson, A. A. Brunette, A. C. McDonnell, K. S. Murray, A. G. Wedd, *J. Am. Chem. Soc.* **1981**, *103*, 1953–1959.
- [9] W. E. Cleland, Jr., K. M. Barnhart, K. Yamanouchi, D. Collison, F. E. Mabbs, R. B. Ortega, J. H. Enemark, *Inorg. Chem.* **1987**, *26*, 1017–1025.
- [10] C. S. J. Chang, D. Collison, F. E. Mabbs, J. H. Enemark, *Inorg. Chem.* **1990**, *29*, 2261–2267.
- [11] M. D. Carducci, C. Brown, E. I. Solomon, J. H. Enemark, *J. Am. Chem. Soc.* **1994**, *116*, 11856–11868.
- [12] P. Basu, M. A. Bruck, Z. Li, I. K. Dhawan, J. H. Enemark, *Inorg. Chem.* **1995**, *34*, 405–407.
- [13] I. K. Dhawan, J. H. Enemark, *Inorg. Chem.* **1996**, *35*, 4873–4882.
- [14] C. Balagopalakrishna, J. T. Kimbrough, T. D. Westmoreland, *Inorg. Chem.* **1996**, *35*, 7758–7768.
- [15] S. Nipales, T. D. Westmoreland, *Inorg. Chem.* **1997**, *36*, 756–757.

- [16] J. Swann, T. D. Westmoreland, *Inorg. Chem.* **1997**, *36*, 5348–5357.
- [17] F. E. Inscore, R. McNaughton, B. L. Westcott, M. E. Helton, R. Jones, I. K. Dhawan, J. H. Enemark, M. L. Kirk, *Inorg. Chem.* **1999**, *38*, 1401–1410.
- [18] C. G. Young, J. H. Enemark, D. Collison, F. E. Mabbs, *Inorg. Chem.* **1987**, *26*, 2925–2927.
- [19] R. Singh, J. T. Spence, G. N. George, S. P. Cramer, *Inorg. Chem.* **1989**, *28*, 8–10.
- [20] G. Backes, J. H. Enemark, T. M. Loehr, *Inorg. Chem.* **1991**, *30*, 1839–1842.
- [21] D. Collison, D. R. Eardley, F. E. Mabbs, K. Rigby, M. A. Bruck, J. H. Enemark, P. A. Wexler, *J. Chem. Soc., Dalton Trans.* **1994**, 1003–1011.
- [22] The structure of $\text{Tp}^*\text{MoOCl}_2$ has been determined and the Cl and O atoms were found to be randomly disordered over the three sites *trans* to the N-donor atoms: G. Ferguson, B. Kaitner, F. J. Lalor, G. Roberts, *J. Chem. Res. (S)* **1982**, 6–7.
- [23] L. J. Laughlin, C. G. Young, *Inorg. Chem.* **1996**, *35*, 1050–1058.
- [24] C. G. Young, L. J. Laughlin, S. Colmanet, S. D. B. Scrofani, *Inorg. Chem.* **1996**, *35*, 5368–5377.
- [25] A. R. Johnson, W. M. Davis, C. C. Cummins, S. Serron, S. P. Nolan, D. G. Musaev, K. Morokuma, *J. Am. Chem. Soc.* **1998**, *120*, 2071–2085.
- [26] A. G. Orpen, L. Brammer, F. H. Allen, O. Kennard, D. G. Watson, R. Taylor, *J. Chem. Soc., Dalton Trans.* **1989**, S1–S83.
- [27] R. W. Gable, J. P. Hill, C. G. Young, unpublished crystallographic study.
- [28] A. A. Eagle, E. R. T. Tiekink, G. N. George, C. G. Young, *Inorg. Chem.* **2001**, *40*, in press.
- [29] P. D. Smith, D. A. Slizys, G. N. George, C. G. Young, *J. Am. Chem. Soc.* **2000**, *122*, 2946–2947.
- [30] G. M. Sheldrick, *SHELXS-86* **1986**, University of Göttingen, Germany.
- [31] G. M. Sheldrick, *SHELXL-97* **1997**, University of Göttingen, Germany.
- [32] C. K. Johnson, *ORTEP*. Report ORNL-5138, Oak Ridge National Laboratory, Oak Ridge, TN, **1976**.
- [33] I. Pickering, G. N. George, *Inorg. Chem.* **1995**, *34*, 3142–3152.

Received January 31, 2001
[I01037]